Supporting Information

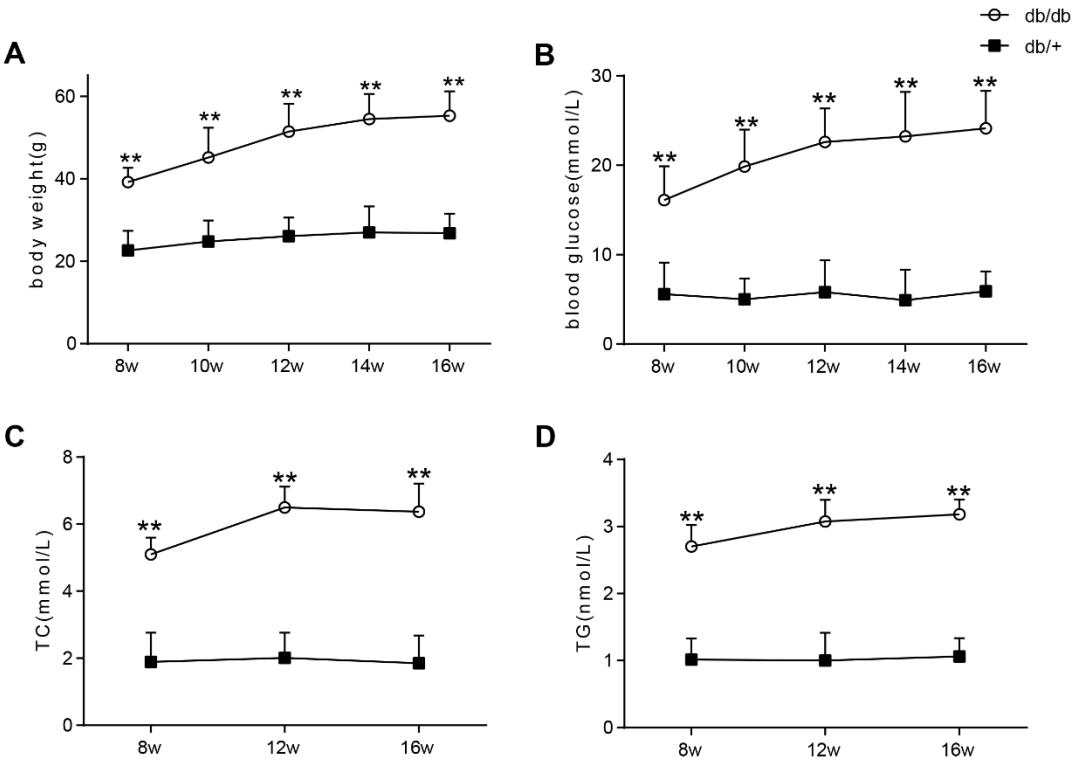

Figure S1 Body weight, blood glucose and serum lipid in db/db and db/+ mice. (A) &(B) Body weight and blood glucose of db/db and db/+ mice were determined every 2 weeks. n=8 animals. (C)&(D) Serum lipids of db/db and db/+ mice were determined every 4 weeks. n=4 animals. ***P*<0.01 vs age-match db/+ mice. TG, triglyceride; TC, total cholesterol.

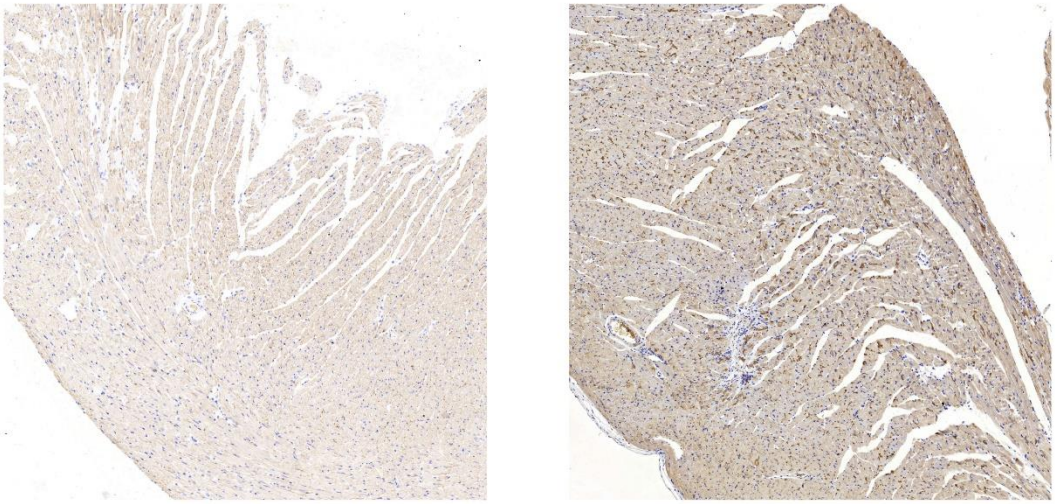

Figure S2 Intramyocardially adenovirus injection achieved transmural expression of Mfn2 in mouse hearts.

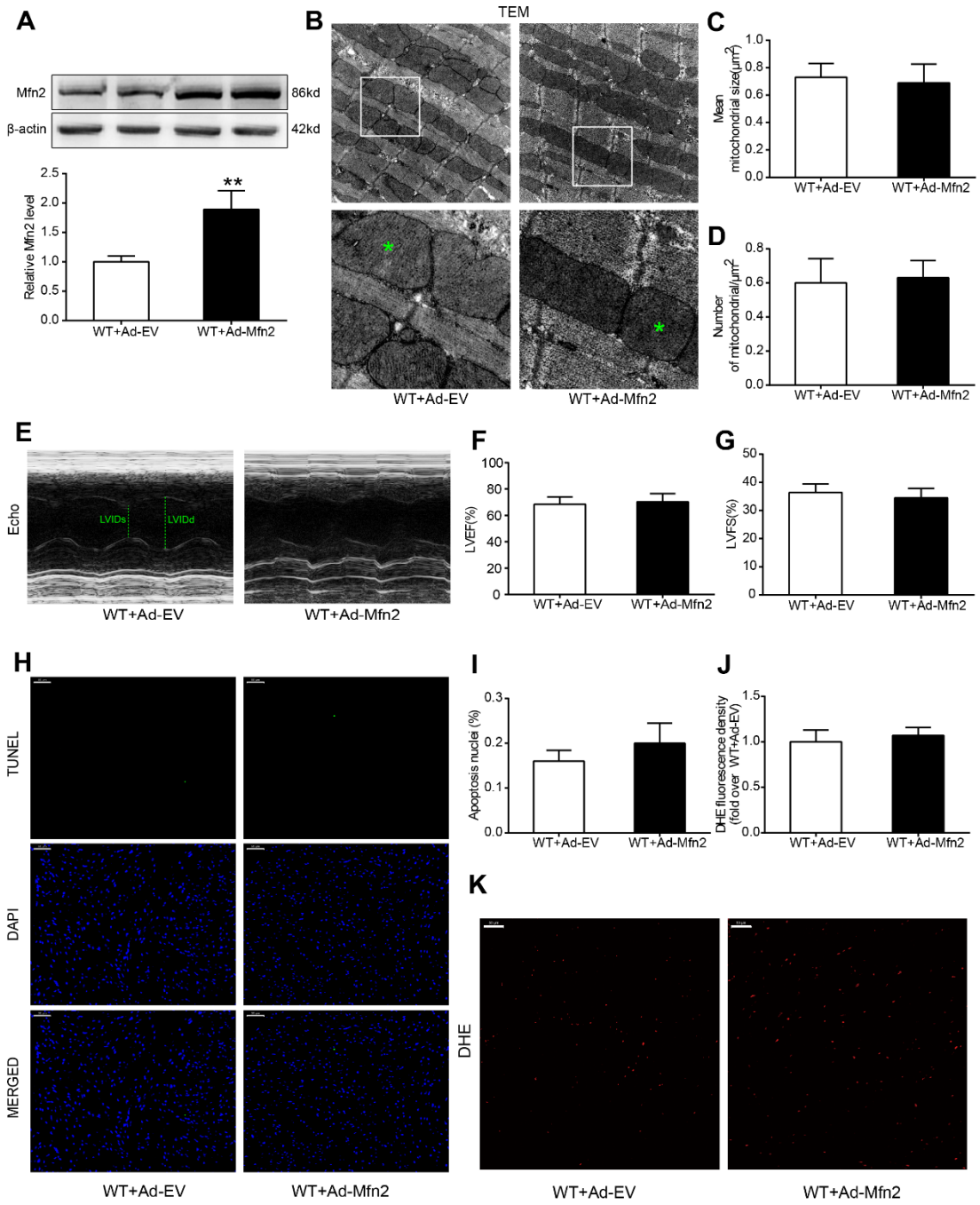

Figure S3 Overexpression of Mfn2 did not have significant effects on mitochondrial morphology, cardiac function, myocardial apoptosis and oxidative stress in WT hearts. (A) Representative blot images and quantitative analysis of Mfn2 expression. (B) Representative transmission electron microscopic images of the myocardium, mitochondria were labeled by asterisks. Scale bars=1 μm. (C) Mean area of mitochondria. (D) The number of mitochondria per um^2. (E) Representative M-mode echocardiography images. LVIDs and LVIDd were labeled. (F) LVEF, left ventricular ejection fraction (G) LVFS, left ventricular fractional shortening. (H)

Representative photomicrographs of TUNEL-stained and DAPI-stained heart sections. Green fluorescence shows TUNEL-positive nuclei; Blue fluorescence shows nuclei of total cardiomyocytes (DAPI-positive). Scale bar = 50 μm. (I) Percentage of TUNEL-positive nuclei. (J) Quantitative analysis of DHE fluorescence density (fold over WT+Ad-EV). (K) Representative microphotographs of DHE staining in heart sections. Scale bar=50 μm. WT, wild type; Ad-Mfn2, recombinant adenovirus encoding Mfn2. n=4-6 animals.

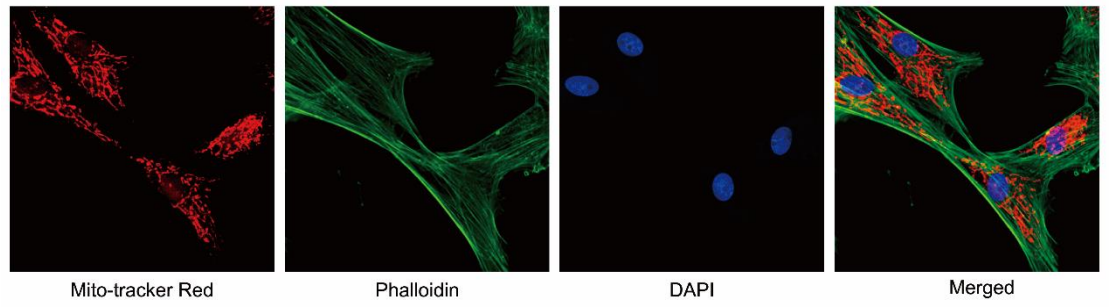

Figure S4 Triple staining of mitochondria, cytoskeleton and nuclear using Mito-tracker red, phalloidin and DAPI respectively in the cardiomyocytes.

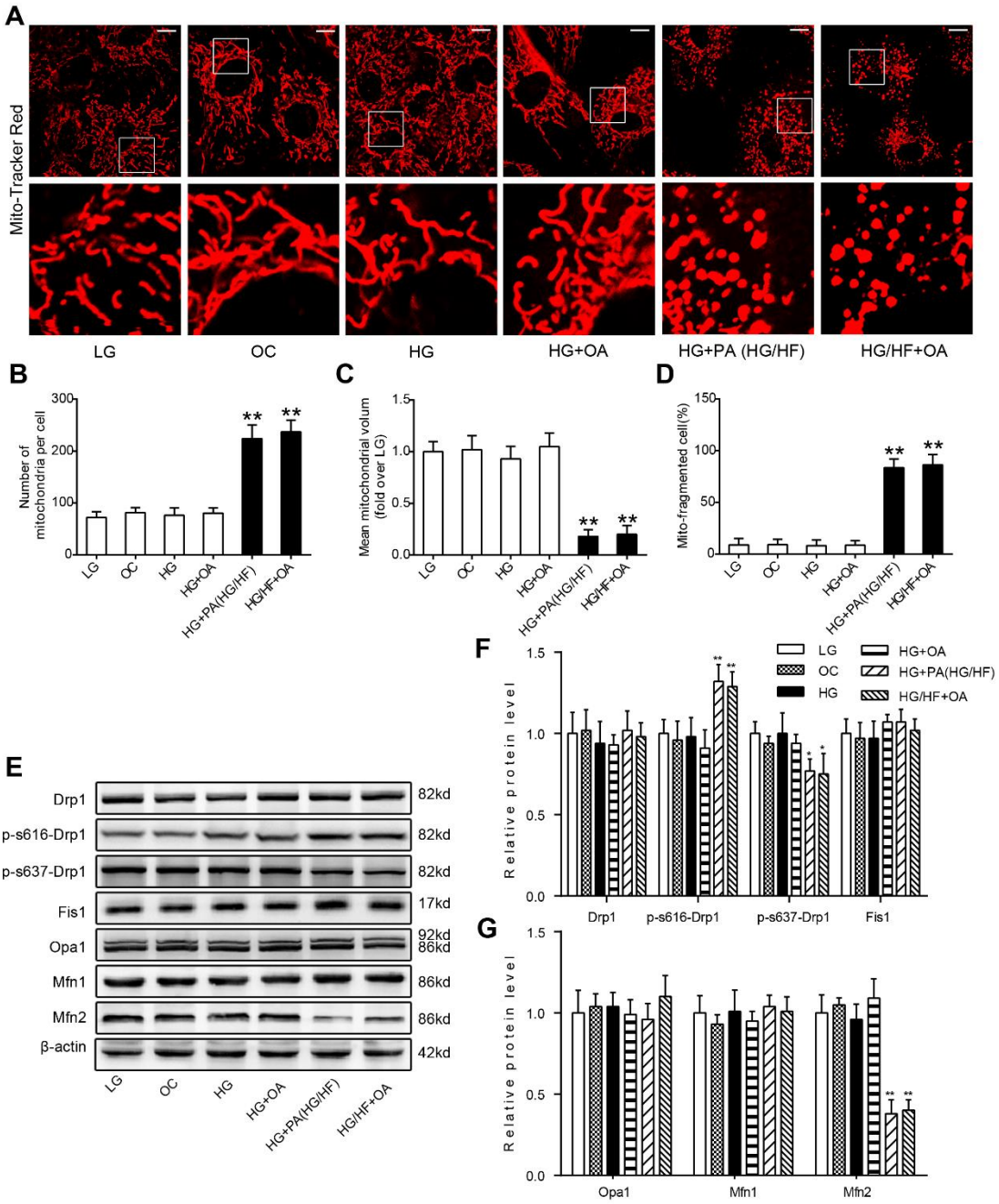

Figure S5 Excessive mitochondrial fission and decreased Mfn2 expression were observed in HG/HF-treated cardiomyocytes. (A) Representative confocal microscope images showing mitochondrial morphology stained by MitoTracker Red. Original magnification ×600. (B) The number of mitochondria in per cell. (C) Mean volume of per mitochondria (fold over LG). (D) The percentage of cells with fragmented mitochondria. (E) Representative blot images of mitochondrial fission-related proteins (Drp1, S-616-Drp1, S-637-Drp1 and Fis1) and fusion-related proteins (Opa1, Mfn1 and Mfn2). (F)&(G) Quantitative analysis of dynamics-related

proteins expression. LG, low glucose (5.5 mmol/L); OC, osmolarity control (5.5 mmol/L glucose and 19.5mmol/L mannitol); HG, high glucose (25mmol/L); HG+OA, HG+ oleate acid (HG+ 500 μmol/L oleate); HG+PA(HG/HF), HG+ palmitate acid (25 mmol/L glucose and 500 μmol/L palmitate); HG/HF+OA, HG/HF+oleate acid (HG/HF+ 500 μmol/L oleate). *P<0.05 vs. HG, **P<0.01 vs. HG. n = 6 in each group.

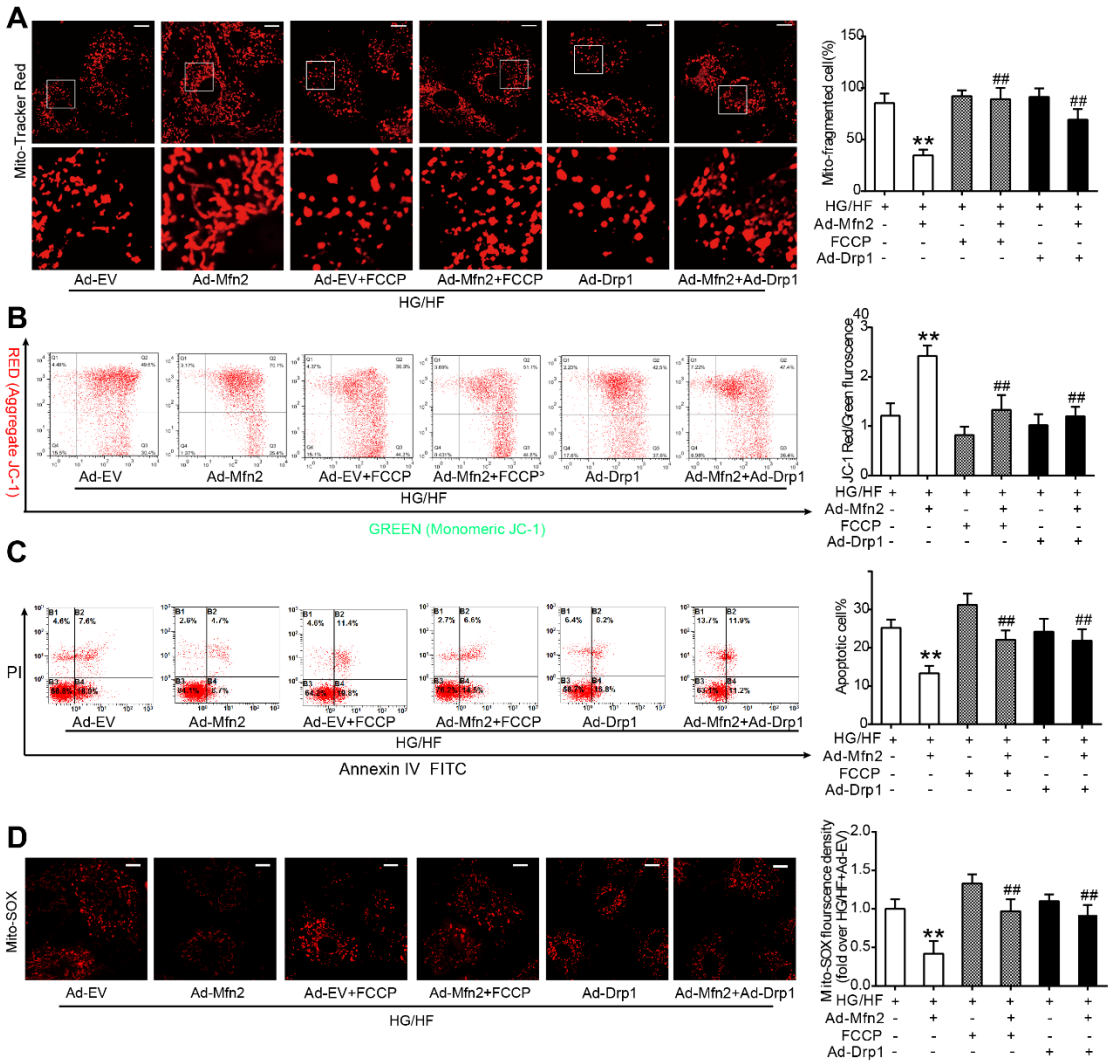

Figure S6. Fission activator FCCP and Drp1 overexpression adenovirus in Mfn2-overexpressed cells blunted the protective effects of Mfn2. (A) Representative confocal microscope images showing mitochondrial morphology stained by MitoTracker Red and percentage of mito-fragmented cells. Original magnification ×600. (B) Flow cytometry and quantitative analysis of mitochondrial membrane potential by JC-1. High levels of green fluorescence (x-axis) represent reduced ΔΨm, and high levels of red fluorescence (y-axis) show increased ΔΨm. A decrease in the red/green fluorescence is indicative of loss of ΔΨm. (C) Flow cytometry and quantitative analysis of apoptosis. (D) Representative confocal microscope images of mitochondria derived superoxide production stained by Mito-SOX and fluorescence quantitation (fold over HG/HF +Ad-EV). Original magnification ×600. Ad-EV, control adenovirus; Ad-Mfn2, recombinant adenovirus

encoding Mfn2; Ad-Drp1, recombinant adenovirus encoding Drp1; HG/HF, high-glucose and high-fat medium. **P<0.01 vs. HG/HF(+Ad-EV), #P<0.05, ##P<0.01 vs. HG/HF + Ad-Mfn2. n = 6 in each group.

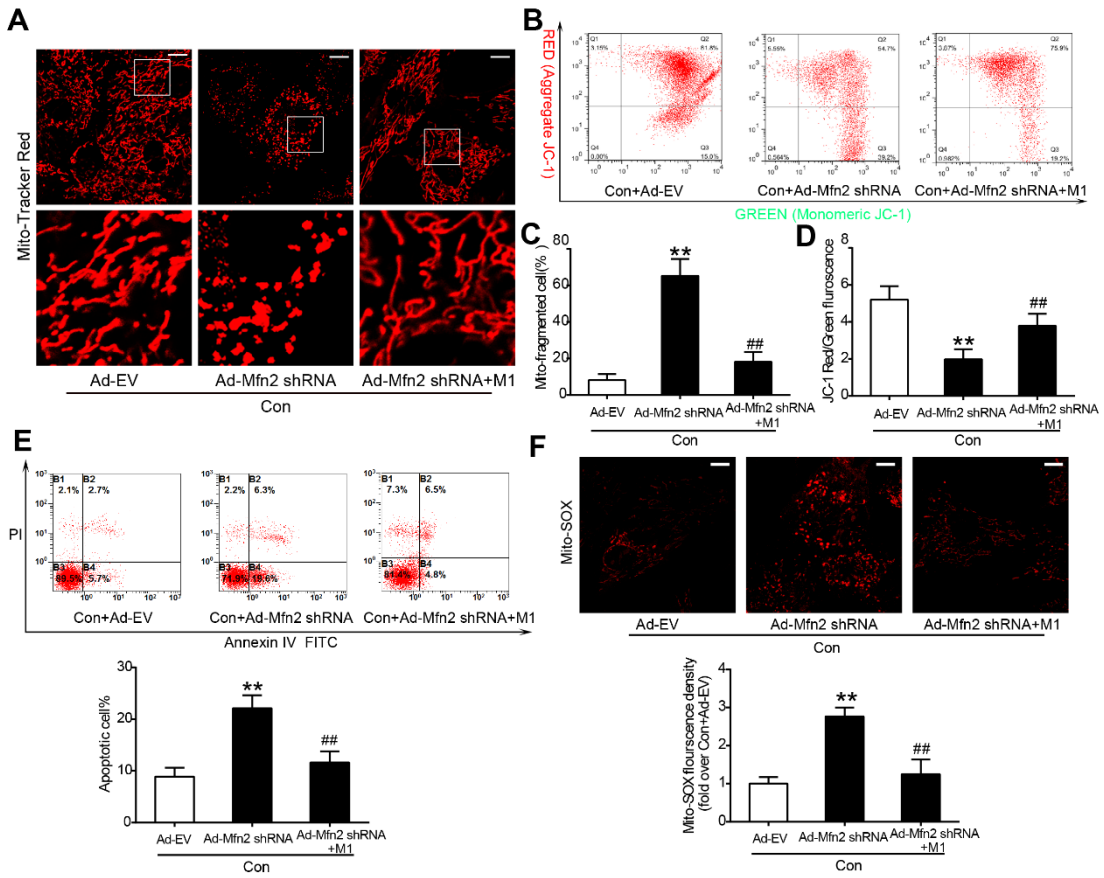

Figure S7 Fusion activator M1 restored mitochondrial fusion and exerted the protective effects in Mfn2-knockdown cardiomyocytes. (A) Representative confocal microscope images showing mitochondrial morphology stained by MitoTracker Red. Original magnification ×600. (B) Flow cytometry analysis of mitochondrial membrane potential by JC-1. High levels of green fluorescence (x-axis) represent reduced ΔΨm, and high levels of red fluorescence (y-axis) show increased ΔΨm. A decrease in the red/green fluorescence is indicative of loss of ΔΨm. (C)Percentage of mito-fragmented cell. (D) Quantification of mitochondrial membrane potential by JC-1. (E) Flow cytometry and quantitative analysis of apoptosis. (F) Representative confocal microscope images of mitochondria derived superoxide production stained by Mito-SOX and fluorescence quantitation (fold over Con+Ad-EV). Original magnification ×600. Ad-EV, control adenovirus; Ad-Mfn2 shRNA, recombinant adenovirus encoding short hairpin RNA against Mfn2. ***P*<0.01 vs. Con + Ad-EV, #*P*<0.05, ##*P*<0.01 vs. Con + Ad-Mfn2 shRNA. n = 6 in each group.

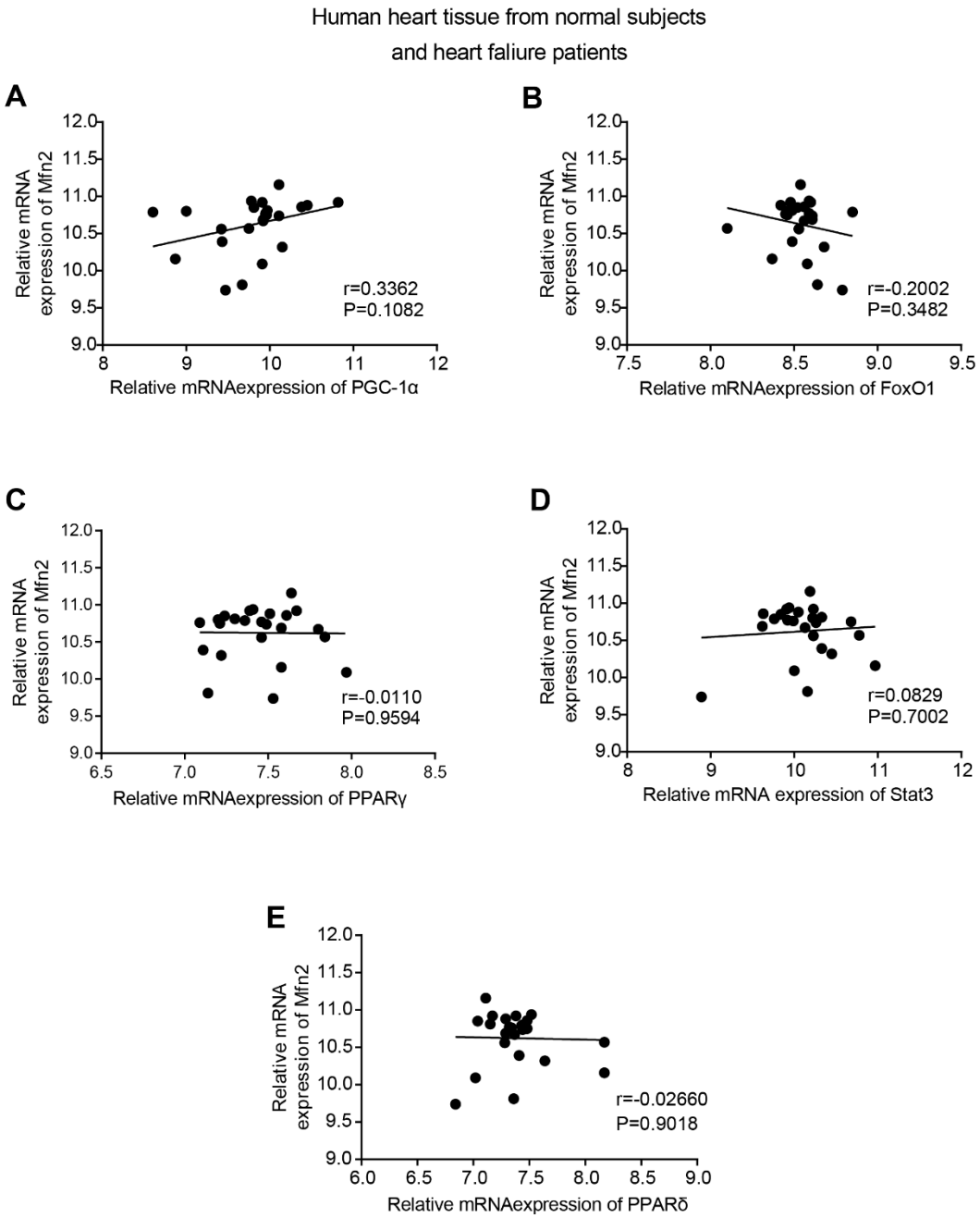

Figure S8 Correlations between the mRNA expression levels of Mfn2 and several potential transcription factors (PGC-1α, FoxO1, PPARγ, Stat3 and PPARδ) in human hearts based on a public microarray expression data set (GSE26887).

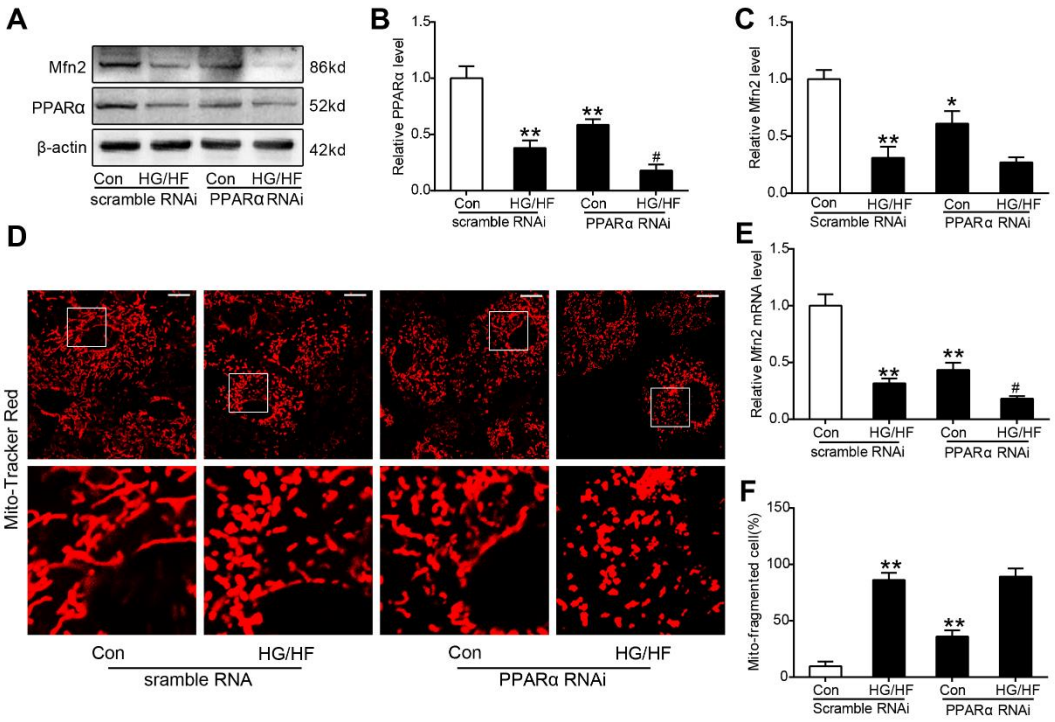

Figure S9 PPARα knockdown inhibited Mfn2 expression and induced mitochondrial fission in cardiomyocytes. (A-C) Representative blot images and quantitative analysis of PPARα and Mfn2 protein expression in primary cardiomyocytes. (D) Representative confocal microscope images showing mitochondrial morphology stained by MitoTracker Red. Original magnification ×600. (E) Real-time PCR analysis of Mfn2 mRNA expression in primary cardiomyocytes. (F) The percentage of cells with fragmented mitochondria. HG/HF, high-glucose and high-fat medium. **P*<0.05 vs. Con + scramble RNAi; ***P*<0.01 vs. Con + scramble RNAi; #*P*<0.05 vs. HG/HF + scramble RNAi. n = 6 in each group.

Full length Mfn2 promoter (-2000~0)

Full length mfn2 promoter(-2000~0), deletion sites were marked.

TTTTAATAATAAATATTGGGGCATCTCTCTACAGCAACTACATTTCAGGTCCT
CAGTAGCTACAGGTGGCTGGTGGGTGTTACTACAGAGCCTAGGCTTGGAGC
ACTCCCAGCTTGGGGTTGTATGCTGTATCCCAGTTCTTGGAACAAAATAAG
AGGCCAGTGAATGACATATGAGCAACTCATCATGCCCCGGGTGTCCTGGGA
CTGCTGTGAAAATTAAAAATTGCATGTTAGATACCCAGCTCAATGACTGTCA
CCTAGTAGGTGCCTGGTGCACTGTGGCTGCTGTTTTGTTGCCTCAAAGGCA
ACTGAAGGACAATTACTTCACCCTAACGGTCTGTTTGTTCCCTTTGAAGAC
ACACTTTCAAATTATGAAACGCAAGTCTGGATTTCAAAGATGACAGGTGTT
ACAGGGTCATGTTCTGGAGCAACAACAACAAAAGGGCACGCAAACCTCTA
ATCCGCACCCTTATCGTTTTTGTGCCGGTCCCCTTCTCCTCTGTCCACCCTCT
CCCCTCCACTCCCCCCCCTTCCCCTTCCCAACCCCTGCTTGACAGCTCGAG
GCTCCGCCCTACCCCACCCTGCCGGGCGCTGGTTCAAACTACAACTCCCAT
GATGCGCTGGGAGCCCCACCCCACAGCTTACGTCATCTGCATAAGACGCGG
GACGGTTATCAGGCACGCGGAGGCTCCTTTTGGAGCGCGGAGTTCCTCGA
CACTGTATAGGAGTGATAGGGTTGAAGTGACGGTGTTCAGAGGCCATCGGT
TCATCCGGGCTTCAGCAGGGCTAGTGACGAGCGCAGCCCCCTCCCCTCCCG
CTTCTCTCAATGTGGCGCTGGCCAGTGACGTGTTGGGTGTGATGGCCGCCG
CGAGGCCGGGAAGGTGAAGGTGAGAGGGCGAGCGCGCTGGGGAGGGGG
AACCGGCAGGCCCCGGCCGGGAGAGTCCTGAGCCACCCGGCTTGGGACG
CTGGGACGCTGGGGCCCCTGGGCCTTGGGCTCAGGCTCCGGTCATACGGG
CTTTTCCCCTGCTCCGGCCTCGCCGCCGGGCCCTCCTCGTCTCTGAGGAGG
GGGCGGGCCACAGGACTCAGGGCTGGGAGGTGGGCTCCTTGGTCTCATTC
CTGACCCCTGCCCCATTCCCGGTTTTCATCCAGTACTTTTCTTTTCTGTTGCC
AGCATCTTTCCAGGACCCAGTACACTGTACCTCACTTACGGTGGAGGTCTT
TTTACTTACATGGCTTCTCATTGCACCGTTAAGACCCCGAGGATTGGAGCTA
TTCTTATCCGTCCCTGACCCTAGCACCTAACACACCGAAAGGCCACAGTAA
TCTCTAAAAAGGACAGCTGATGAAGAAAGGCAAAGCTGTTGGCCTCCATC
TCTTGTAATACTTTTATCCTGTTTTCCTTTCCGGATCATCGCTCCTTCTGTCA
GAAAAGGACTCTTGATGCCCCAACCCCCTCTTGTCTTATGTAGGAAAACAA
AGCGAGCTTTAACAAAGCGAGCTTTAGAGTCACAGCTAGTGTATTTTGGTG
TCTAGCTTGGCTACTTGACTTTCTACATCTTCCTAGTACTCCAGGGGACAAG
TTTACTCCATAGACTTGAATGGAAGGGGATACTTTATAGCATCAGGGACACT
CTGGCTTTTATCAGGTCTAATACTCTTCCTCTCCATGCCCCTTCCATTTCTAG
TTGGCAGTTTCCCAGTCCTCAAGGCCAGGCCTTGTCCTGATTCTGATCCCTT
CTCTCTCTCTGACTGTGCCTTTGCAAAGACCTCTTTGGTGCTTTAGCACATG
GCTAATGTGTGCGCGAGCACACCTGTGCTTTGTGTCCTTGTCATTGTTGTTT
TTTCCTCCTCCCCCTCCACACTTCCTCACCTGCTCCCGAAGCACCTCAATGA
GTAAGCTTCCCTCAGGGATGTGTTAGTTTGGCTTAACACCTCATTAGGCATA
GTTTGCATTTTCTTTCCTGGTTGCCCAGTTGACCTCTCCCTTTTCCTTTCCAA